AIMS Mathematics

https://www.aimspress.com/journal/Math

AIMS Mathematics, 11(9): 30065–30090.
DOI:10.3934/math.20261191
Received: 01 July 2026
Revised: 02 September 2026
Accepted: 04 September 2026
Published: 16 September 2026

Research article

Stability and bifurcation analysis of a discrete-time predator-prey model with combined effects of prey harvesting and anti-predator behavior

Asifa Tassaddiq[1], Youngsoo Seol[2,*], Rabab Alharbi[3], Ruhaila Md. Kasmani[4] and Rizwan Ahmed[5]

[1] Department of Information Technology, College of Computer and Information Sciences, Majmaah University, Al Majmaah 11952, Saudi Arabia

[2] Department of Mathematics, Dong-A University, Busan 49315, Republic of Korea

[3] Department of Mathematics, College of Science, Qassim University, Buraydah 51452, Saudi Arabia

[4] Institute of Mathematical Sciences, Universiti Malaya, Kuala Lumpur 50603, Malaysia

[5] International Center for Interdisciplinary Research in Sciences, The University of Lahore, Lahore 54792, Pakistan

* **Correspondence:** Email: prosul76@dau.ac.kr.

Abstract: This work focuses on examining the joint influence of prey harvesting and anti-predator responses within a discrete-time predator-prey model. Beginning with a continuous formulation, the model is converted into a discrete system via the forward Euler scheme, allowing the representation of stepwise ecological dynamics and enabling more complex behavioral patterns to emerge. The presence and local stability of equilibrium states are investigated using the Jacobian matrix alongside eigenvalue-based criteria. In addition, the emergence of transcritical, period-doubling (PD), and Neimark–Sacker (NS) bifurcations is systematically derived through normal forms and center manifold theory. To support the analytical results, numerical simulations, such as bifurcation plots and computations of the maximum Lyapunov exponent, are conducted. The findings show that the system is capable of exhibiting a rich dynamic behavior, such as periodic behavior, quasi-periodic phenomena, and chaotic dynamics, through changes in the values of parameters. Specifically, the combined effect of prey harvesting intensity and anti-predation strategies plays an important role in the stability of the system and can either increase or disrupt stability. It is pointed out that an increased environmental carrying capacity or unbalanced parameter selection might cause chaotic population dynamics.

Keywords: predator-prey system; stability; bifurcation; chaos; Lyapunov exponent; simulation
Mathematics Subject Classification: 39A28, 39A30

1. Introduction

Predator-prey models are an essential part of mathematical biology used to describe species interactions and analyze the processes that determine their population dynamics. Such models can be used to study interspecific competition and coevolution in the ecological environment. The classical predator-prey model by Lotka–Volterra [1, 2] represents a simple example of this class of models. Nevertheless, natural ecosystems exhibit a much greater variety of dynamical properties due to environmental changes. For example, fluctuations in fish populations and their predators in marine ecosystems, or the interaction between wolves and deer in forest environments, demonstrate how predator-prey relationships can lead to oscillations, stabilization, or sudden collapse depending on ecological conditions. Such observations highlight the need for more realistic models that incorporate additional biological and environmental factors, as demonstrated by recent studies incorporating mechanisms such as Allee effects, fear effects, opportunistic predation, and spatial diffusion [3–5].

Among these factors, harvesting has received considerable attention because human activities such as fishing and hunting can directly modify prey abundance and indirectly influence predator populations through changes in food availability. Mathematical studies have shown that harvesting can significantly affect coexistence and stability and may also generate different types of bifurcations. For example, Kumar and Kharbanda [6] considered nonlinear prey harvesting together with group defense and reported saddle-node and Hopf bifurcations, while Suryanto et al. [7] investigated linear harvesting in a fractional-order predator-prey model and established conditions for existence, boundedness, stability, and Hopf bifurcation. Mortuja et al. [8] showed that nonlinear prey harvesting below the maximum sustainable yield can support coexistence, whereas excessive harvesting may destabilize the system. Panigoro et al. [9] reported period-doubling (PD) bifurcation and chaotic dynamics in a fractional-order discrete model with proportional harvesting. Similarly, Imran et al. [10] identified PD and Neimark–Sacker (NS) bifurcations in a discrete predator-prey system with harvesting, whereas Eskandari et al. [11] demonstrated that predator harvesting may lead to flip and strong resonance bifurcations. Singh et al. [12] investigated a discretized predator-prey model incorporating harvesting and prey refuge and reported NS and PD bifurcations together with multistability, chaotic dynamics, Arnold tongues, and complex periodic structures. These studies indicate that harvesting acts not only as a population-removal mechanism but also as an important parameter governing qualitative changes in ecological dynamics.

Anti-predator behavior provides another mechanism through which prey populations can influence predator-prey interactions. Prey may reduce predation risk through refuge use, group formation, defensive behavior, camouflage, or other protective strategies. Such responses can reduce the effectiveness of predation and consequently influence predator growth and population persistence. Several mathematical formulations have been proposed to represent these effects. Tang and Xiao [13] studied anti-predator behavior in which prey attack predators and showed that such behavior can suppress oscillations and modify coexistence through bifurcations. Prasad and Prasad [14] examined the combined influence of additional food and anti-predator behavior and reported complex dynamical responses. Saha and Samanta [15] incorporated anti-predator behavior together with a strong Allee effect and showed that sufficiently strong defensive behavior can reduce the predator population and generate complicated bifurcation structures. Wang and Li [16] investigated anti-predator effects in a fractional-order framework and obtained Hopf, NS, and PD bifurcations, while Wen et al. [17]

demonstrated that the interaction between Allee effects and anti-predator behavior can produce higher-codimension bifurcations and multiple limit cycles. Collectively, these works demonstrate that defensive responses of prey can substantially alter coexistence and the qualitative behavior of predator-prey systems.

Motivated by these ecological considerations, we consider the following predator-prey system:

$$\begin{cases} \dfrac{\mathrm{d}x}{\mathrm{d}t} = rx\left(1 - \dfrac{x}{k}\right) - \alpha xy - \epsilon x, \\ \dfrac{\mathrm{d}y}{\mathrm{d}t} = y\left(\beta x - \gamma - \eta x\right), \end{cases} \tag{1.1}$$

where $x(t)$ and $y(t)$ denote prey and predator populations, respectively. The prey grows logistically with intrinsic growth rate r and carrying capacity k, while α represents the predation rate. The term ϵx represents proportional harvesting of the prey population, where ϵ denotes the per-capita harvesting rate. In the predator equation, β denotes the conversion efficiency, while γ is the natural death rate. The parameter η represents the anti-predator effect and is interpreted as an aggregate measure of the inhibitory influence of prey defense on predator growth rather than as an explicit representation of a particular mechanism such as refuge use or group defense. This simplified formulation allows us to investigate how changes in the overall strength of prey defense influence the qualitative dynamics of the predator-prey interaction. All parameters are positive real numbers.

Although continuous-time models provide valuable theoretical insight, many ecological processes evolve in discrete time. For example, breeding seasons in animals, periodic harvesting cycles in fisheries, and annual data collection in population studies naturally occur at discrete intervals. As a result, discrete-time models are often more appropriate for describing such systems. Moreover, discretization can lead to richer dynamical behavior, including oscillations, bifurcations, and chaos, which are not usually present in continuous models [18–20]. Such characteristics make discrete models particularly suitable for examining how variations in model parameters influence qualitative dynamics.

To investigate these dynamical features, system (1.1) is discretized using the forward Euler method [21, 22]. The resulting discrete model takes the following form:

$$\begin{cases} x_{n+1} = x_n + h\left(rx_n\left(1 - \dfrac{x_n}{k}\right) - \alpha x_n y_n - \epsilon x_n\right), \\ y_{n+1} = y_n + hy_n\left(\beta x_n - \gamma - \eta x_n\right), \end{cases} \tag{1.2}$$

where $h > 0$ represents the step size. This discrete formulation allows us to investigate how prey harvesting and anti-predator effects influence the emergence of complex population dynamics.

Some previous studies have investigated the combined influence of harvesting and anti-predator behavior mainly within continuous-time predator-prey models [23–25]. These studies have demonstrated that the interaction of these ecological factors can substantially affect population coexistence and stability. Motivated by these findings, the present work examines how prey harvesting and anti-predation jointly influence the dynamics of a discrete predator-prey system. Our main objective is to determine their effects on the existence and stability of the fixed points and to identify the parameter conditions under which qualitative changes in the system dynamics occur. In particular, the discrete formulation enables the investigation of dynamical transitions associated with transcritical, PD, and NS bifurcations and the subsequent emergence of periodic, quasiperiodic, and chaotic behavior. Thus, rather than claiming novelty solely from combining harvesting and anti-predation, the present study focuses on how their interaction influences stability switching and complex dynamical transitions in the discrete-time setting.

The remainder of the paper is organized as follows. In Section 2, we examine fixed points' existence and stability. Bifurcation analysis is presented in Section 3. Numerical simulations and sensitivity analysis are performed in Section 4. Conclusions are drawn in Section 5.

2. Existence and local stability analysis of fixed points

In this section, we investigate the existence and local stability of the fixed points of system (1.2). Local stability is determined from the eigenvalues of the Jacobian matrix evaluated at each fixed point, providing insight into the behavior of nearby population trajectories.

The fixed points (x, y) for the system (1.2) can be obtained by solving

$$\begin{cases} x = x + h\left(rx\left(1 - \dfrac{x}{k}\right) - \alpha xy - \epsilon x\right), \\ y = y + hy\left(\beta x - \gamma - \eta x\right). \end{cases} \tag{2.1}$$

The discrete system (1.2) admits three fixed points, namely

$$E_0 = (0, 0),\ E_1 = \left(k - \frac{k\epsilon}{r}, 0\right),\ E^* = \left(\frac{\gamma}{\beta - \eta}, \frac{k(\beta - \eta)(r - \epsilon) - \gamma r}{\alpha k(\beta - \eta)}\right).$$

The trivial fixed point E_0 always exists. The boundary fixed point E_1 exists only if $r > \epsilon$. E^* is the unique positive fixed point only if $\beta > \eta,\ r > \epsilon$, and $k > \frac{\gamma r}{(\beta-\eta)(r-\epsilon)}$.

Biologically, the equilibrium E_0 refers to the extinction equilibrium point, where both prey and predator populations become extinct. This can happen in cases where there are unfavorable environmental conditions or heavy harvesting activities. Equilibrium E_1 refers to a situation where predators are absent, meaning that the prey population survives at a low population size due to harvesting. This may be caused by a reduction in predator populations due to the absence of sufficient prey or anti-predator measures. The coexistence equilibrium E^* is of primary ecological importance, as it reflects a stable balance between prey growth, predation, harvesting, and anti-predator effects. The feasibility conditions for E^* indicate that predator survival requires sufficient prey availability and that harvesting must remain below a critical threshold.

The classification of fixed points is carried out using the same methodology employed in [26–28]. Through simple computations, one can obtain the Jacobian matrix at an arbitrary fixed point (x, y) as follows:

$$J(x, y) = \begin{bmatrix} 1 + h(r - \frac{2rx}{k} - y\alpha - \epsilon) & -hx\alpha \\ hy(\beta - \eta) & 1 - h(\gamma + x(-\beta + \eta)) \end{bmatrix}.$$

We get

$$J(E_0) = \begin{bmatrix} 1 + h(r - \epsilon) & 0 \\ 0 & 1 - h\gamma \end{bmatrix}.$$

Theorem 2.1. E_0 *is*

1) A sink if $r < \epsilon,\ h < \frac{2}{\epsilon - r}$, and $\gamma < \frac{2}{h}$.

2) A source whenever either of the following requirements is fulfilled:

   (i) $r < \epsilon, h > \frac{2}{\epsilon - r}$, and $\gamma > \frac{2}{h}$,

   (ii) $r > \epsilon$ and $\gamma > \frac{2}{h}$.

3) A saddle whenever any of the following conditions holds:

   (i) $r < \epsilon,\ h > \frac{2}{\epsilon - r}$, and $\gamma < \frac{2}{h}$,

   (ii) $r > \epsilon$ and $\gamma < \frac{2}{h}$,

   (iii) $r < \epsilon,\ h < \frac{2}{\epsilon - r}$, and $\gamma > \frac{2}{h}$.

4) Nonhyperbolic whenever either of the following requirements is met:

   (i) $r = \epsilon$,

   (ii) $\gamma = \frac{2}{h}$,

   (iii) $r < \epsilon$ and $h = \frac{2}{\epsilon - r}$.

We obtain

$$J(E_1) = \begin{bmatrix} 1 + h(-r + \epsilon) & -\frac{hk\alpha(r-\epsilon)}{r} \\ 0 & 1 - h\gamma + \frac{hk(r-\epsilon)(\beta-\eta)}{r} \end{bmatrix}.$$

Theorem 2.2. E_1 *is*

1) A sink if $h < \frac{2}{r - \epsilon}$ and $\frac{k(r-\epsilon)(\beta-\eta)}{r} < \gamma < \frac{2}{h} + \frac{k(r-\epsilon)(\beta-\eta)}{r}$.

2) A source if $h > \frac{2}{r - \epsilon}$ and either of the following is satisfied:

   (i) $\gamma < \frac{k(r-\epsilon)(\beta-\eta)}{r}$,

   (ii) $\gamma > \frac{2}{h} + \frac{k(r-\epsilon)(\beta-\eta)}{r}$.

3) A saddle if any of the following is met:

   (i) $h > \frac{2}{r-\epsilon}$ and $\frac{k(r-\epsilon)(\beta-\eta)}{r} < \gamma < \frac{2}{h} + \frac{k(r-\epsilon)(\beta-\eta)}{r}$,

   (ii) $h < \frac{2}{r-\epsilon}$ and $\gamma < \frac{k(r-\epsilon)(\beta-\eta)}{r}$,

   (iii) $h < \frac{2}{r-\epsilon}$ and $\gamma > \frac{2}{h} + \frac{k(r-\epsilon)(\beta-\eta)}{r}$.

4) Nonhyperbolic if either of the following is met:

   (i) $h = \frac{2}{r-\epsilon}$,

   (ii) $\gamma = \frac{k(r-\epsilon)(\beta-\eta)}{r}$,

   (iii) $\gamma = \frac{2}{h} + \frac{k(r-\epsilon)(\beta-\eta)}{r}$.

Next, the Jacobian matrix at the positive fixed point E^* is

$$J(E^*) = \begin{bmatrix} 1 + \frac{hr\gamma}{k(-\beta+\eta)} & \frac{h\alpha\gamma}{-\beta+\eta} \\ \frac{h(-r\gamma+k(r-\epsilon)(\beta-\eta))}{k\alpha} & 1 \end{bmatrix}. \tag{2.2}$$

The associated characteristic polynomial is

$$\Lambda(\xi) = \xi^2 + K_1\xi + K_0,$$

where

$$K_1 = -2 + \frac{hr\gamma}{k\beta - k\eta}, \; K_0 = 1 + h\gamma\Big(h(r-\epsilon) - \frac{r(1+h\gamma)}{k(\beta-\eta)}\Big).$$

It can be obtained through calculations that

$$\Lambda(0) = 1 + h\gamma\Big(h(r-\epsilon) - \frac{r(1+h\gamma)}{k(\beta-\eta)}\Big), \; \Lambda(-1) = 4 + h\gamma\Big(h(r-\epsilon) - \frac{r(2+h\gamma)}{k(\beta-\eta)}\Big), \; \Lambda(1) = h^2\gamma\Big(r - \epsilon - \frac{r\gamma}{k(\beta-\eta)}\Big).$$

Since the existence of E^* requires $\beta > \eta, \; r > \epsilon$, and $k > \frac{\gamma r}{(\beta-\eta)(r-\epsilon)}$, these conditions imply that $\Lambda(1) > 0$. Hence, we obtain the following result.

Theorem 2.3. *E^* is*

1) A sink if $\frac{hr\gamma(2+h\gamma)}{(\beta-\eta)(4+h^2\gamma(r-\epsilon))} < k < \frac{r(1+h\gamma)}{h(\beta-\eta)(r-\epsilon)}$.

2) A source if $k > \max\left\{\frac{hr\gamma(2+h\gamma)}{(\beta-\eta)(4+h^2\gamma(r-\epsilon))}, \frac{r(1+h\gamma)}{h(\beta-\eta)(r-\epsilon)}\right\}$.

3) A saddle if $k < \frac{hr\gamma(2+h\gamma)}{(\beta-\eta)(4+h^2\gamma(r-\epsilon))}$.

4) Nonhyperbolic, and (1.2) goes through PD bifurcation at E^* when

$$\frac{hr\gamma}{k(\beta-\eta)} \neq 2, 4 \quad \text{and} \quad k = \frac{hr\gamma(2+h\gamma)}{(\beta-\eta)(4+h^2\gamma(r-\epsilon))}.$$

5) Nonhyperbolic, and (1.2) goes through NS bifurcation at E^* when

$$0 < \frac{hr\gamma}{k(\beta-\eta)} < 4 \quad \text{and} \quad k = \frac{r(1+h\gamma)}{h(\beta-\eta)(r-\epsilon)}.$$

3. Bifurcation analysis

This section investigates the local bifurcations of system (1.2). Transcritical and PD bifurcations are considered at the boundary fixed point E_1, while PD and NS bifurcations are studied at the positive fixed point E^*. The corresponding critical conditions are derived by varying appropriate system parameters. For the theoretical background on discrete bifurcation analysis, we refer to [29–31].

3.1. Transcritical bifurcation at E_1

We investigate the transcritical bifurcation at E_1 based on condition (4–*ii*) as presented in Theorem 2.2. By applying a small perturbation δ to the bifurcation parameter γ around the critical value

$$\gamma_1 = \frac{k(r-\epsilon)(\beta-\eta)}{r},\ \beta > \eta,$$

the system (1.2) is changed to

$$\begin{cases} x_{n+1} = x_n + h\left(rx_n\left(1-\dfrac{x_n}{k}\right) - \alpha x_n y_n - \epsilon x_n\right), \\ y_{n+1} = y_n + hy_n\left(\beta x_n - (\gamma_1+\delta) - \eta x_n\right). \end{cases} \tag{3.1}$$

For the local analysis of E_1, we shift this fixed point to the origin using the following transformation:

$$u_n = x_n - k + \frac{k\epsilon}{r},\ v_n = y_n.$$

As a result, the system (3.1) is transformed into the following form:

$$\begin{bmatrix} u_{n+1} \\ v_{n+1} \end{bmatrix} = \begin{bmatrix} 1+h(-r+\epsilon) & \frac{hk\alpha(-r+\epsilon)}{r} \\ 0 & 1 \end{bmatrix} \begin{bmatrix} u_n \\ v_n \end{bmatrix} + \begin{bmatrix} F(u_n,v_n,\delta) \\ G(u_n,v_n,\delta) \end{bmatrix}, \tag{3.2}$$

where

$$F(u_n,v_n,\delta) = -\frac{hr}{k}u_n^2 - h\alpha u_n v_n,\ G(u_n,v_n,\delta) = h(\beta-\eta)u_n v_n - hv_n\delta.$$

Next, system (3.2) is diagonalized using the following transformation:

$$\begin{bmatrix} u_n \\ v_n \end{bmatrix} = \begin{bmatrix} -\frac{k\alpha}{r} & 1 \\ 1 & 0 \end{bmatrix} \begin{bmatrix} e_n \\ f_n \end{bmatrix}. \tag{3.3}$$

Using the transformation (3.3), system (3.2) can be rewritten as

$$\begin{bmatrix} e_{n+1} \\ f_{n+1} \end{bmatrix} = \begin{bmatrix} 1 & 0 \\ 0 & 1+h(-r+\epsilon) \end{bmatrix} \begin{bmatrix} e_n \\ f_n \end{bmatrix} + \begin{bmatrix} \Gamma(e_n,f_n,\delta) \\ \Upsilon(e_n,f_n,\delta) \end{bmatrix}, \tag{3.4}$$

where

$$\begin{aligned} \Gamma(e_n,f_n,\delta) &= \frac{hk\alpha(-\beta+\eta)}{r}e_n^2 + h(\beta-\eta)e_n f_n - he_n\delta, \\ \Upsilon(e_n,f_n,\delta) &= \frac{hk^2\alpha^2(-\beta+\eta)}{r^2}e_n^2 - \frac{hr}{k}f_n^2 + \frac{h\alpha(r+k(\beta-\eta))}{r}e_n f_n - \frac{hk\alpha}{r}e_n\delta. \end{aligned}$$

Next, let Q^C denote the center manifold of system (3.4) at the origin in a small neighborhood of $\delta = 0$. It can be expressed as follows:

$$Q^C = \left\{(e_n,f_n,\delta) \in \mathbb{R}_+^3 \,\middle|\, f_n = p_1 e_n^2 + p_2 e_n\delta + p_3\delta^2 + O((|e_n|+|\delta|)^3)\right\}.$$

Through computations, we obtain

$$p_1=\frac{k^2\alpha^2(-\beta+\eta)}{r^2(r-\epsilon)},\ p_2=\frac{k\alpha}{r(-r+\epsilon)},\ p_3=0.$$

Therefore, restricting system (3.4) to the center manifold Q^C gives

$$\Phi(e_n,\delta)=e_{n+1}=e_n+\frac{hk\alpha(-\beta+\eta)}{r}e_n^2-he_n\delta-\frac{hk^2\alpha^2(\beta-\eta)^2}{r^2(r-\epsilon)}e_n^3+\frac{hk\alpha(\beta-\eta)}{r(-r+\epsilon)}e_n^2\delta+O\Big((|e_n|+|\delta|)^4\Big). \tag{3.5}$$

Using simple calculations, we get

$$\begin{aligned}&\Phi(0,0)=0,\ \Phi_{e_n}(0,0)=1,\ \Phi_{\delta}(0,0)=0,\\ &\Phi_{e_ne_n}(0,0)=\frac{2hk\alpha(-\beta+\eta)}{r}\neq 0,\ \Phi_{e_n\delta}(0,0)=-h\neq 0.\end{aligned}$$

As a result, we obtain the following result.

Theorem 3.1. *If requirement* (4–*ii*) *in Theorem 2.2 is satisfied, then* (1.2) *goes through transcritical bifurcation at E_1 if γ varies within a small neighborhood of $\gamma_1=\frac{k(r-\epsilon)(\beta-\eta)}{r}$.*

3.2. PD bifurcation at E_1

We investigate the PD bifurcation at E_1 based on condition (4–*i*) as presented in Theorem 2.2. By applying a small perturbation δ to the bifurcation parameter h around the critical value $h_1=\frac{2}{r-\epsilon}$, the system (1.2) is changed to

$$\begin{cases}x_{n+1}=x_n+(h_1+\delta)\left(rx_n\left(1-\frac{x_n}{k}\right)-\alpha x_ny_n-\epsilon x_n\right),\\ y_{n+1}=y_n+(h_1+\delta)y_n\left(\beta x_n-\gamma-\eta x_n\right).\end{cases} \tag{3.6}$$

To study the dynamics near E_1, we shift the fixed point to the origin through the following change of variables:

$$u_n=x_n-k+\frac{k\epsilon}{r},\ v_n=y_n.$$

As a result, the system (3.6) is transformed into the following form:

$$\begin{bmatrix}u_{n+1}\\ v_{n+1}\end{bmatrix}=\begin{bmatrix}-1 & -\frac{2k\alpha}{r}\\ 0 & 1-\frac{2\gamma}{r-\epsilon}+\frac{2k(\beta-\eta)}{r}\end{bmatrix}\begin{bmatrix}u_n\\ v_n\end{bmatrix}+\begin{bmatrix}F(u_n,v_n,\delta)\\ G(u_n,v_n,\delta)\end{bmatrix}, \tag{3.7}$$

where

$$\begin{aligned}F(u_n,v_n,\delta)&=-\frac{2r}{kr-k\epsilon}u_n^2-\frac{2\alpha}{r-\epsilon}u_nv_n+(-r+\epsilon)u_n\delta+\frac{k\alpha(-r+\epsilon)}{r}v_n\delta-\frac{r}{k}u_n^2\delta-\alpha u_nv_n\delta,\\ G(u_n,v_n,\delta)&=\frac{2(\beta-\eta)}{r-\epsilon}u_nv_n+\Big(-\gamma+\frac{k(r-\epsilon)(\beta-\eta)}{r}\Big)v_n\delta+(\beta-\eta)u_nv_n\delta.\end{aligned}$$

Next, we diagonalize system (3.7) using the following transformation:

$$\begin{bmatrix} u_n \\ v_n \end{bmatrix} = \begin{bmatrix} 1 & -\frac{k\alpha(r-\epsilon)}{r^2+kr\beta-r\gamma-r\epsilon-k\beta\epsilon-kr\eta+k\epsilon\eta} \\ 0 & 1 \end{bmatrix} \begin{bmatrix} e_n \\ f_n \end{bmatrix}. \tag{3.8}$$

Applying transformation (3.8) to system (3.7) gives

$$\begin{bmatrix} e_{n+1} \\ f_{n+1} \end{bmatrix} = \begin{bmatrix} -1 & 0 \\ 0 & 1+\frac{2\gamma}{-r+\epsilon}+\frac{2k(\beta-\eta)}{r} \end{bmatrix} \begin{bmatrix} e_n \\ f_n \end{bmatrix} + \begin{bmatrix} \Gamma(e_n, f_n, \delta) \\ \Upsilon(e_n, f_n, \delta) \end{bmatrix}, \tag{3.9}$$

where

$$\Gamma(e_n, f_n, \delta) = c_1 e_n^2 + c_2 f_n^2 + c_3 e_n f_n + c_4 e_n \delta + c_5 e_n^2 \delta + c_6 f_n^2 \delta + c_7 e_n f_n \delta,$$
$$\Upsilon(e_n, f_n, \delta) = d_1 f_n^2 + d_2 e_n f_n + d_3 f_n \delta + d_4 f_n^2 \delta + d_5 e_n f_n \delta,$$

$$c_1 = -\frac{2r}{kr-k\epsilon},\ c_2 = -\frac{2kr\alpha^2\gamma}{\left(r^2+k\epsilon(-\beta+\eta)-r(\gamma+\epsilon+k(-\beta+\eta))\right)^2},$$

$$c_3 = \frac{2r\alpha(r+\gamma-\epsilon)}{(r-\epsilon)\left(r^2+k\epsilon(-\beta+\eta)-r(\gamma+\epsilon+k(-\beta+\eta))\right)},\ c_4 = -r+\epsilon,\ c_5 = -\frac{r}{k},$$

$$c_6 = \frac{kr\alpha^2\gamma(-r+\epsilon)}{\left(r^2+k\epsilon(-\beta+\eta)-r(\gamma+\epsilon+k(-\beta+\eta))\right)^2},\ c_7 = \frac{r\alpha(r+\gamma-\epsilon)}{r^2+k\epsilon(-\beta+\eta)-r(\gamma+\epsilon+k(-\beta+\eta))},$$

$$d_1 = -\frac{2k\alpha(\beta-\eta)}{r^2+k\epsilon(-\beta+\eta)-r(\gamma+\epsilon+k(-\beta+\eta))},\ d_2 = \frac{2(\beta-\eta)}{r-\epsilon},$$

$$d_3 = -\gamma+\frac{k(r-\epsilon)(\beta-\eta)}{r},\ d_4 = -\frac{k\alpha(r-\epsilon)(\beta-\eta)}{r^2+k\epsilon(-\beta+\eta)-r(\gamma+\epsilon+k(-\beta+\eta))},\ d_5 = \beta-\eta.$$

Next, let Q^C denote the center manifold of system (3.9) at the origin in a small neighborhood of $\delta = 0$. It can be expressed as follows:

$$Q^C = \left\{ (e_n, f_n, \delta) \in \mathbb{R}_+^3 \middle| f_n = p_1 e_n^2 + p_2 e_n \delta + p_3 \delta^2 + O((|e_n| + |\delta|)^3) \right\}.$$

Through computations, we obtain $p_1 = p_2 = p_3 = 0$. As a result, the system (3.9) is limited to Q^C in the manner as follows:

$$\tilde{F} := e_{n+1} = -e_n - \frac{2r}{kr-k\epsilon} e_n^2 + (-r+\epsilon) e_n \delta - \frac{r}{k} e_n^2 \delta + O\Big((|e_n| + |\delta|)^4\Big). \tag{3.10}$$

For the function (3.10) to go through PD bifurcation, the following two quantities must be nonzero:

$$l_1 = \tilde{F}_\delta \tilde{F}_{e_n e_n} + 2\tilde{F}_{e_n \delta}\Big|_{(0,0)} = 2(-r+\epsilon) \neq 0, \tag{3.11}$$

$$l_2 = \frac{1}{2}(\tilde{F}_{e_n e_n})^2 + \frac{1}{3}\tilde{F}_{e_n e_n e_n}\Big|_{(0,0)} = \frac{8r^2}{(kr-k\epsilon)^2} \neq 0. \tag{3.12}$$

The preceding analysis leads to the next result.

Theorem 3.2. *Assume that condition* (4–*i*) *of Theorem 2.2 holds true. The system* (1.2) *experiences PD bifurcation at* E_1 *if h fluctuates in a close neighborhood of* $h_1 = \frac{2}{r-\epsilon}$. *Moreover, since* $l_2 > 0$, *a period-2 orbit of the system* (1.2) *emerges from* E_1, *and it is stable.*

Remark 3.3. *A similar bifurcation analysis can be carried out at* E_0. *In particular, a transcritical bifurcation may occur when condition* (4–*i*) *of Theorem 2.1 holds, while a PD bifurcation may occur when condition* (4–*ii*) *or* (4–*iii*) *is satisfied.*

3.3. PD bifurcation at E^*

The PD bifurcation at E^* is examined using condition (4) of Theorem 2.3. Adding a small change δ into k around $k_1 = \frac{hr\gamma(2+h\gamma)}{(\beta-\eta)(4+h^2\gamma(r-\epsilon))}$, (1.2) becomes

$$\begin{cases} x_{n+1} = x_n + h\left(rx_n\left(1 - \dfrac{x_n}{(k_1+\delta)}\right) - \alpha x_n y_n - \epsilon x_n\right), \\ y_{n+1} = y_n + hy_n\left(\beta x_n - \gamma - \eta x_n\right). \end{cases} \tag{3.13}$$

We translate E^* to $(0,0)$ by setting

$$u_n = x_n - \frac{\gamma}{\beta-\eta},\ v_n = y_n - \frac{(k_1+\delta)(\beta-\eta)(r-\epsilon)-\gamma r}{\alpha(k_1+\delta)(\beta-\eta)}.$$

Consequently, we obtain

$$\begin{bmatrix} u_{n+1} \\ v_{n+1} \end{bmatrix} = \begin{bmatrix} \frac{-2+h\gamma+h^2\gamma(-r+\epsilon)}{2+h\gamma} & -\frac{h\alpha\gamma}{\beta-\eta} \\ \frac{2(-2+h(r-\epsilon))(\beta-\eta)}{\alpha(2+h\gamma)} & 1 \end{bmatrix} \begin{bmatrix} u_n \\ v_n \end{bmatrix} + \begin{bmatrix} \mathbb{F}_1(u_n,v_n,\delta) \\ \mathbb{F}_2(u_n,v_n,\delta) \end{bmatrix}, \tag{3.14}$$

where

$$\begin{aligned} \mathbb{F}_1(u_n,v_n,\delta) &= a_1u_n^2 + a_2u_nv_n + a_3u_n\delta + a_4u_n^2\delta + a_5u_n\delta^2 + O(4), \\ \mathbb{F}_2(u_n,v_n,\delta) &= b_1u_nv_n + b_2u_n\delta + b_3u_n\delta^2 + O(4), \end{aligned}$$

$$a_1 = -\frac{(4+h^2\gamma(r-\epsilon))(\beta-\eta)}{\gamma(2+h\gamma)},\ a_2 = -h\alpha,\ a_3 = \frac{(4+h^2\gamma(r-\epsilon))^2(\beta-\eta)}{hr\gamma(2+h\gamma)^2},\ a_4 = \frac{(4+h^2\gamma(r-\epsilon))^2(\beta-\eta)^2}{hr\gamma^2(2+h\gamma)^2},$$

$$a_5 = -\frac{(4+h^2\gamma(r-\epsilon))^3(\beta-\eta)^2}{h^2r^2\gamma^2(2+h\gamma)^3},\ b_1 = h(\beta-\eta),\ b_2 = \frac{(4+h^2\gamma(r-\epsilon))^2(\beta-\eta)^2}{hr\alpha\gamma(2+h\gamma)^2},\ b_3 = -\frac{(4+h^2\gamma(r-\epsilon))^3(\beta-\eta)^3}{h^2r^2\alpha\gamma^2(2+h\gamma)^3}.$$

The system (3.14) is then diagonalized using the transformation given by

$$\begin{bmatrix} u_n \\ v_n \end{bmatrix} = \begin{bmatrix} -\frac{2\alpha+h\alpha\gamma}{(-2+hr-h\epsilon)(\beta-\eta)} & -\frac{h\alpha\gamma}{2(\beta-\eta)} \\ 1 & 1 \end{bmatrix} \begin{bmatrix} e_n \\ f_n \end{bmatrix}. \tag{3.15}$$

By applying (3.15), (3.14) transforms to

$$\begin{bmatrix} e_{n+1} \\ f_{n+1} \end{bmatrix} = \begin{bmatrix} -1 & 0 \\ 0 & \frac{2+h\gamma(3+h(-r+\epsilon))}{2+h\gamma} \end{bmatrix} \begin{bmatrix} e_n \\ f_n \end{bmatrix} + \begin{bmatrix} \mathbb{G}_1(e_n,f_n,\delta) \\ \mathbb{G}_2(e_n,f_n,\delta) \end{bmatrix}, \tag{3.16}$$

where

$$\mathbb{G}_1(e_n, f_n, \delta) = c_1 e_n^2 + c_2 f_n^2 + c_3 e_n f_n + c_4 e_n \delta + c_5 f_n \delta + c_6 e_n^2 \delta + c_7 f_n^2 \delta + c_8 e_n \delta^2 + c_9 f_n \delta^2 + c_{10} e_n f_n \delta + O(4),$$
$$\mathbb{G}_2(e_n, f_n, \delta) = d_1 e_n^2 + d_2 f_n^2 + d_3 e_n f_n + d_4 e_n \delta + d_5 f_n \delta + d_6 e_n^2 \delta + d_7 f_n^2 \delta + d_8 e_n \delta^2 + d_9 f_n \delta^2 + d_{10} e_n f_n \delta + O(4).$$

The values of c_i and d_j are listed in Appendix A. Let Q^C be the center manifold of (3.16) at the origin near $\delta = 0$, which can be computed as

$$Q^C = \left\{ (e_n, f_n, \delta) \in \mathbb{R}_+^3 \middle| f_n = p_1 e_n^2 + p_2 e_n \delta + p_3 \delta^2 + O(3) \right\}.$$

Through computations, we obtain

$$p_1 = \frac{2\alpha(2 + h\gamma)^4}{h\gamma^2(-4 + h\gamma(-4 + h(r - \epsilon)))(2 + h(-r + \epsilon))^2},\ p_2 = \frac{2(4 + h^2\gamma(r - \epsilon))^2(r + \gamma - \epsilon)(\beta - \eta)}{r\gamma(-2 + h(r - \epsilon))(4 + h\gamma(4 + h(-r + \epsilon)))^2},\ p_3 = 0.$$

Hence, the restriction of system (3.16) to Q^C is

$$\tilde{F} := e_{n+1} = q_1 e_n + q_2 e_n^2 + q_3 e_n \delta + q_4 e_n^3 + q_5 e_n^2 \delta + q_6 e_n \delta^2 + O(4), \tag{3.17}$$

where

$$q_1 = -1,\ q_2 = -\frac{\alpha(2 + h\gamma)(8 + h\gamma(4 + h\gamma(-2 + h(r - \epsilon))))}{\gamma(-4 + h\gamma(-4 + h(r - \epsilon)))(-2 + h(r - \epsilon))},$$

$$q_3 = -\frac{(4 + h^2\gamma(r - \epsilon))^2(\beta - \eta)}{hr\gamma(-4 + h\gamma(-4 + h(r - \epsilon)))},\ q_4 = -\frac{\alpha^2(2 + h\gamma)^5(4 + h^2\gamma(r - \epsilon))}{\gamma^2(2 + h(-r + \epsilon))^2(4 + h\gamma(4 + h(-r + \epsilon)))^2},$$

$$\begin{aligned} q_5 = &-\Big(\alpha(4 + h^2\gamma(r - \epsilon))^2(-64 + h\gamma(-144 + 32h(r - 3\gamma - \epsilon) + h^4\gamma^2(r - \epsilon)(r + 2\gamma - \epsilon) - 4h^3\gamma^2(-2r + \gamma + 2\epsilon) \\ &- 8h^2\gamma(-4r + 3\gamma + 4\epsilon)))(\beta - \eta)\Big)\Big/\Big(hr\gamma^2(-4 + h\gamma(-4 + h(r - \epsilon)))^3(-2 + h(r - \epsilon))\Big), \end{aligned}$$

$$q_6 = -\frac{(-8 + h\gamma(-12 + h(6 + h\gamma)(r - \epsilon)))(4 + h^2\gamma(r - \epsilon))^3(\beta - \eta)^2}{h^2 r^2 \gamma^2(-4 + h\gamma(-4 + h(r - \epsilon)))^3}.$$

For the function (3.17) to undergo PD bifurcation, it is required that the following two values are non-zero:

$$l_1 = \tilde{F}_\delta \tilde{F}_{e_n e_n} + 2\tilde{F}_{e_n \delta}\Big|_{(0,0)} = -\frac{2(4 + h^2\gamma(r - \epsilon))^2(\beta - \eta)}{hr\gamma(-4 - 4h\gamma + h^2\gamma(r - \epsilon))}, \tag{3.18}$$

$$l_2 = \frac{1}{2}(\tilde{F}_{e_n e_n})^2 + \frac{1}{3}\tilde{F}_{e_n e_n e_n}\Big|_{(0,0)} = \frac{2\alpha^2(2 + h\gamma)^2(-8 + 4h\gamma + 6h^2\gamma^2 - h^3\gamma^3 + h^4\gamma^3(r - \epsilon))}{\gamma^2(-2 + h(r - \epsilon))^2(-4 - 4h\gamma + h^2\gamma(r - \epsilon))}. \tag{3.19}$$

From the previous discussion, we obtain the next conclusion.

Theorem 3.4. *Assume that requirement* (4) *of Theorem 2.3 is fulfilled. The system* (1.2) *undergoes PD bifurcation at E^* if l_1, l_2 given in* (3.18) *and* (3.19) *are non-zero and k varies in a close neighbourhood of $k_1 = \frac{hr\gamma(2+h\gamma)}{(\beta-\eta)(4+h^2\gamma(r-\epsilon))}$. Moreover, if $l_2 > 0$ (respectively, $l_2 < 0$), then a period-2 orbit of* (1.2) *emanates from E^*, and it is stable (respectively, unstable).*

3.4. NS bifurcation at E^*

We investigate the NS bifurcation at E^* when condition (5) of Theorem 2.3 is satisfied. Introducing a small perturbation δ to the bifurcation parameter k around the critical value $k_2 = \frac{r(1+h\gamma)}{h(\beta-\eta)(r-\epsilon)}$ in (1.2), we obtain

$$\begin{cases} x_{n+1} = x_n + h\left(rx_n\left(1 - \dfrac{x_n}{(k_2+\delta)}\right) - \alpha x_n y_n - \epsilon x_n\right), \\ y_{n+1} = y_n + hy_n\left(\beta x_n - \gamma - \eta x_n\right). \end{cases} \tag{3.20}$$

We use the translation $u_n = x_n - \frac{\gamma}{\beta-\eta}$, $v_n = y_n - \frac{(k_2+\delta)(\beta-\eta)(r-\epsilon)-\gamma r}{\alpha(k_2+\delta)(\beta-\eta)}$ to translate E^* to $(0,0)$. As a result, (3.20) can be written as

$$\begin{bmatrix} u_{n+1} \\ v_{n+1} \end{bmatrix} = \begin{bmatrix} m_{11} & m_{12} \\ \frac{h(\beta-\eta)(r-\epsilon+\frac{hr\gamma(-r+\epsilon)}{r+hr(\gamma+\delta(\beta-\eta))+h\delta\epsilon(-\beta+\eta)})}{\alpha} & 1 \end{bmatrix} \begin{bmatrix} u_n \\ v_n \end{bmatrix} + \begin{bmatrix} F(u_n, v_n) \\ G(u_n, v_n) \end{bmatrix}, \tag{3.21}$$

where

$$m_{11} = 1 + \frac{h^2 r\gamma(-r+\epsilon)}{r + h\delta\epsilon(-\beta+\eta) + hr(\gamma+\beta\delta-\delta\eta)},\ m_{12} = \frac{h\alpha\gamma}{-\beta+\eta},$$

$$F(u_n, v_n) = -\frac{hr}{\delta + \frac{r(1+h\gamma)}{h(r-\epsilon)(\beta-\eta)}} u_n^2 - h\alpha u_n v_n, \quad G(u_n, v_n) = h(\beta-\eta)u_n v_n.$$

The Jacobian matrix of (3.21), determined at the origin, yields the following characteristic equation:

$$\xi^2 - p(\delta)\xi + q(\delta) = 0, \tag{3.22}$$

where

$$p(\delta) = 2 - \frac{h^2 r\gamma(r-\epsilon)}{r + h\delta\epsilon(-\beta+\eta) + hr(\gamma+\beta\delta-\delta\eta)},$$

$$q(\delta) = \frac{r + hr(\gamma+\delta(\beta-\eta)) + h^3 r^2\gamma\delta(\beta-\eta) + h\delta\epsilon(-1+h^2\gamma\epsilon)(\beta-\eta) + 2h^3 r\gamma\delta\epsilon(-\beta+\eta)}{r + hr(\gamma+\delta(\beta-\eta)) + h\delta\epsilon(-\beta+\eta)}.$$

The solutions of (3.22) are given by

$$\xi_{1,2} = \frac{p(\delta)}{2} \pm \frac{i}{2}\sqrt{4q(\delta) - p^2(\delta)}. \tag{3.23}$$

We then obtain

$$|\xi_{1,2}| = \sqrt{q(\delta)}.$$

Differentiating with respect to δ, we have

$$\frac{d|\xi_{1,2}|}{d\delta} = \frac{q'(\delta)}{2\sqrt{q(\delta)}}.$$

At $\delta = 0$, it follows that

$$q(0) = 1, \qquad q'(0) = \frac{h^3\gamma(r-\epsilon)^2(\beta-\eta)}{r+hr\gamma}.$$

Therefore,

$$\left(\frac{d|\xi_1|}{d\delta}\right)_{\delta=0} = \left(\frac{d|\xi_2|}{d\delta}\right)_{\delta=0} = \frac{h^3\gamma(r-\epsilon)^2(\beta-\eta)}{2(r+hr\gamma)} > 0.$$

Hence, the transversality condition for the NS bifurcation is satisfied. Furthermore, it is necessary that $\xi^i_{1,2} \neq 1$ at $\delta = 0$ for $i = 1, 2, 3, 4$, which is similar to $p(0) \neq -2, -1, 0, 2$. We check that

$$p(0) = 2 + \frac{h^2\gamma(-r+\epsilon)}{1+h\gamma} \neq \pm 2.$$

Thus, we only require $p(0) \neq -1, 0$. This is equivalent to

$$r \neq \frac{2}{h} + \frac{2}{h^2\gamma} + \epsilon,\ \frac{3}{h} + \frac{3}{h^2\gamma} + \epsilon. \tag{3.24}$$

To determine the canonical form of (3.21) at $\delta = 0$, we use the following transformation that is constructed from the real and imaginary parts of the eigenvector associated with the complex conjugate eigenvalues of the linearized system of (3.21) at the NS bifurcation point

$$\begin{bmatrix} u_n \\ v_n \end{bmatrix} = \begin{bmatrix} m_{12} & 0 \\ \mu - m_{11} & -\nu \end{bmatrix} \begin{bmatrix} e_n \\ f_n \end{bmatrix}, \tag{3.25}$$

where $\mu = \frac{p(0)}{2}$ and $\nu = \frac{\sqrt{4q^2(0)-p(0)}}{2}$. The determinant of the transformation matrix is $-m_{12}\nu$, which is nonzero. Hence, the transformation is regular and invertible. This transformation takes the following form:

$$\begin{bmatrix} u_n \\ v_n \end{bmatrix} = \begin{bmatrix} \frac{h\alpha\gamma}{-\beta+\eta} & 0 \\ \frac{h^2\gamma(r-\epsilon)}{2+2h\gamma} & j_{22} \end{bmatrix} \begin{bmatrix} e_n \\ f_n \end{bmatrix}, \tag{3.26}$$

where $j_{22} = -\frac{1}{2}\sqrt{4 - (-2 + \frac{h^2\gamma(r-\epsilon)}{1+h\gamma})^2}$. Under the transformation (3.26), (3.21) is transformed to

$$\begin{bmatrix} e_{n+1} \\ f_{n+1} \end{bmatrix} = \begin{bmatrix} \frac{2+h\gamma(2+h(-r+\epsilon))}{2+2h\gamma} & j_{22} \\ -j_{22} & \frac{2+h\gamma(2+h(-r+\epsilon))}{2+2h\gamma} \end{bmatrix} \begin{bmatrix} e_n \\ f_n \end{bmatrix} + \begin{bmatrix} \chi(e_n, f_n) \\ \Upsilon(e_n, f_n) \end{bmatrix}, \tag{3.27}$$

where

$$\chi(e_n, f_n) = \frac{h^3\alpha\gamma(r-\epsilon)}{2+2h\gamma}e_n^2 + h\alpha j_{22} e_n f_n,$$

$$\Upsilon(e_n, f_n) = \frac{h^4\alpha\gamma^2(2+h(r+2\gamma-\epsilon))(r-\epsilon)}{4(1+h\gamma)^2 j_{22}}e_n^2 - \frac{h^2\alpha\gamma(2+h(-r+2\gamma+\epsilon))}{2+2h\gamma}e_n f_n.$$

To determine the direction of the NS bifurcation, we compute the first Lyapunov coefficient, which is obtained as follows:

$$L = \left(\left[-Re\left(\frac{(1-2\xi_1)\xi_2^2}{1-\xi_1}\tau_{20}\tau_{11}\right) - \frac{1}{2}|\tau_{11}|^2 - |\tau_{02}|^2 + Re(\xi_2\tau_{21})\right]\right)_{\delta=0}, \tag{3.28}$$

where

$$\begin{aligned}
\tau_{20} &= \frac{1}{8}\left[\chi_{e_ne_n} - \chi_{f_nf_n} + 2\Upsilon_{e_nf_n} + i(\Upsilon_{e_ne_n} - \Upsilon_{f_nf_n} - 2\chi_{e_nf_n})\right],\\
\tau_{11} &= \frac{1}{4}\left[\chi_{e_ne_n} + \chi_{f_nf_n} + i(\Upsilon_{e_ne_n} + \Upsilon_{f_nf_n})\right],\\
\tau_{02} &= \frac{1}{8}\left[\chi_{e_ne_n} - \chi_{f_nf_n} - 2\Upsilon_{e_nf_n} + i(\Upsilon_{e_ne_n} - \Upsilon_{f_nf_n} + 2\chi_{e_nf_n})\right],\\
\tau_{21} &= \frac{1}{16}\left[\chi_{e_ne_ne_n} + \chi_{e_nf_nf_n} + \Upsilon_{e_ne_nf_n} + \Upsilon_{f_nf_nf_n} + i(\Upsilon_{e_ne_ne_n} + \Upsilon_{e_nf_nf_n} - \chi_{e_ne_nf_n} - \chi_{f_nf_nf_n})\right].
\end{aligned}$$

In light of the preceding analysis, the following result is established.

Theorem 3.5. *Suppose that condition* (5) *of Theorem 2.3 is fulfilled. If condition* (3.24) *is satisfied and L given in* (3.28) *is non-zero, then the system* (1.2) *experiences NS bifurcation at E^*, as long as the parameter k changes in a close neighborhood of $k_2 = \frac{r(1+h\gamma)}{h(\beta-\eta)(r-\epsilon)}$. Furthermore, if $L < 0$ (or $L > 0$), the NS bifurcation at E^* is classified as supercritical (or subcritical), and a single closed invariant curve bifurcates from E^*, which is attracting (or repelling).*

4. Numerical simulations

In this section, we illustrate the analytical results through numerical simulations. The purpose of these simulations is to verify the theoretical results and illustrate complex dynamics of the system (1.2). All numerical calculations are done using MATHEMATICA, whereas graphical illustrations are obtained using MATLAB. The parameter sets used in the numerical simulations are selected hypothetically to satisfy the analytically derived stability and bifurcation conditions and to illustrate the different dynamical regimes of the model.

4.1. Parameter sensitivity

Parameter sensitivity analysis provides a systematic framework to assess how variations in model parameters affect the behavior of a dynamical system. In many real-world models, particularly in ecology and economics, the system response depends strongly on parameter values, making it essential to identify the most influential parameters. To quantify this effect, a normalized sensitivity measure is often used, which compares the relative change in a system output with respect to a relative change in a parameter. For any parameter p, the sensitivity index is

$$S_p = \frac{p}{\bar{x}}\frac{\partial \bar{x}}{\partial p},$$

where $\bar{x}$ denotes an equilibrium value or any significant output variable of the system.

The explanation for S_p is quite clear. If the S_p value is positive, then the response is directly proportional to the parameter; otherwise, the response is inversely proportional to the parameter. In addition, the effect on system behavior becomes more significant with parameters whose absolute values of S_p are greater. On the other hand, smaller absolute values of S_p, especially close to zero, mean that the system does not react much to variations in that particular parameter.

Figure 1 shows sensitivity indices of coexistence equilibrium E^* for three distinct parametric sets. The three cases correspond to parameter sets: (i) $\alpha = 0.55, \beta = 1, \gamma = 0.42, \eta = 0.35, \epsilon = 0.1, h = 0.25, r = 1.4$, and $k = 3.5$, (ii) $\alpha = 0.4, \beta = 0.8, \gamma = 0.3, \eta = 0.1, \epsilon = 0.05, h = 0.3, r = 1$, and $k = 7$, and (iii) $\alpha = 0.7, \beta = 1.25, \gamma = 0.6, \eta = 0.45, \epsilon = 0.2, h = 0.18, r = 1.6$, and $k = 4$. The upper panels (a)–(c) represent the prey component $\bar{x}$ (blue bars), while the lower panels (d)–(f) correspond to the predator component $\bar{y}$ (red bars).

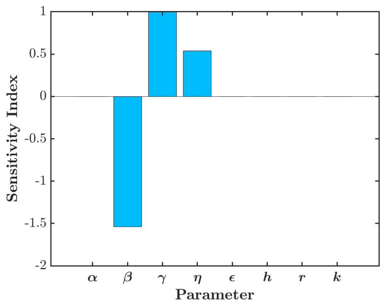

(a) Prey equilibrium sensitivity

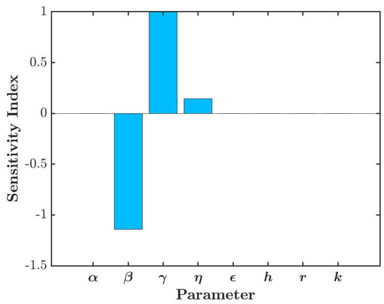

(b) Prey equilibrium sensitivity

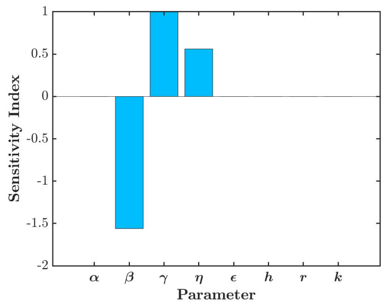

(c) Prey equilibrium sensitivity

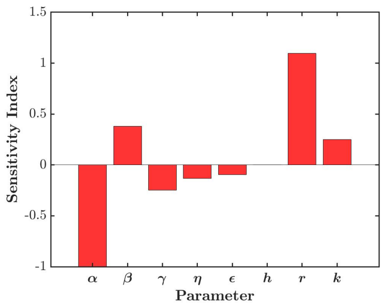

(d) Predator equilibrium sensitivity

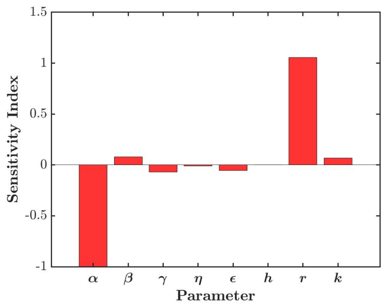

(e) Predator equilibrium sensitivity

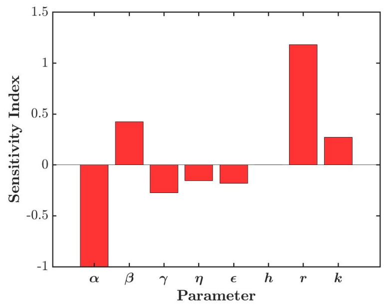

(f) Predator equilibrium sensitivity

Figure 1. Sensitivity analysis of the positive equilibrium E^* for three parameter sets (i)–(iii). (a)–(c) Prey sensitivity indices; (d)–(f) predator sensitivity indices.

From panels (a)–(c), it is clear that the prey equilibrium is mainly influenced by the parameters β, γ, and η. In particular, β has a strong negative effect, meaning that higher conversion efficiency leads to a decrease in prey density. In contrast, γ has a strong positive effect, indicating that an increase in predator mortality increases prey equilibrium. The parameter η also contributes positively, showing that the defensive effect of the prey supports its population. The remaining parameters have negligible impact on $\bar{x}$.

For the predator component shown in panels (d)–(f), the behavior is somewhat different. The parameter α has a strong negative influence, while β, r, and k show clear positive effects on the predator equilibrium. This suggests that predator density increases with higher prey growth and better environmental support. The effects of γ, η, and ϵ are comparatively smaller, although they still play a role in shaping the dynamics.

The findings show that prey equilibrium depends more on interaction parameters while predator equilibrium depends on predation efficiency and environment factors. This will be useful in determining the crucial parameters that affect the dynamics of the system.

4.2. Bifurcation analysis at E_1

We fix the parameter values $\alpha = 0.85, \beta = 0.65, \eta = 0.35, \epsilon = 0.5, h = 0.9, r = 2.5$, and $k = 4.5$. For these parameter values, the critical value for the transcritical bifurcation is $\gamma_1 = 1.08$. At $\gamma = \gamma_1$, the corresponding boundary fixed point is $E_1 = (3.6, 0)$, and the eigenvalues of $J(E_1)$ are $\xi_1 = -0.8$ and $\xi_2 = 1$. The bifurcation diagrams in Figure 2 are obtained by varying $\gamma \in [1.05, 1.15]$. For $\gamma < 1.08$, the positive fixed point E^* is stable, whereas E_1 is unstable. At $\gamma = 1.08$, the fixed points E_1 and E^* coincide and exchange stability. For $\gamma > 1.08$, E_1 becomes stable, while E^* leaves the biologically feasible region.

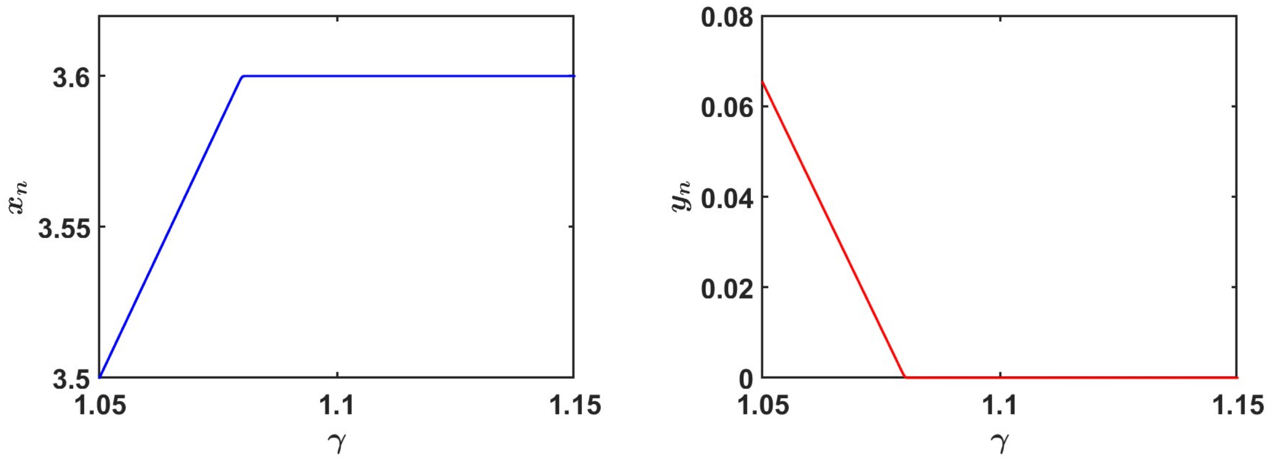

(a) Bifurcation diagram for x_n **(b)** Bifurcation diagram for y_n

Figure 2. Bifurcation diagrams of (1.2) showing transcritical bifurcation at E_1 varying $\gamma \in [1.05, 1.15]$. Fixed parameter values are $\alpha = 0.85, \beta = 0.65, \eta = 0.35, \epsilon = 0.5, h = 0.9, r = 2.5$, and $k = 4.5$, and initial values are $x_0 = 0.5, y_0 = 0.5$.

Next, we fix $\alpha = 0.85$, $\beta = 0.65$, $\gamma = 1.15$, $\eta = 0.35$, $\epsilon = 0.5$, $r = 2.25$, and $k = 4.5$. For these parameter values, the critical value for the PD bifurcation is $h_1 = 1.14286$. At $h = h_1$, the corresponding boundary fixed point is $E_1 = (3.5, 0)$, and the eigenvalues of $J(E_1)$ are $\xi_1 = -1$ and $\xi_2 = 0.885714$. Figure 3(a) shows the bifurcation diagram for x_n, while Figure 3(b) shows the corresponding maximum Lyapunov exponent (MLE) plot. Positive values of the MLE indicate chaotic dynamics.

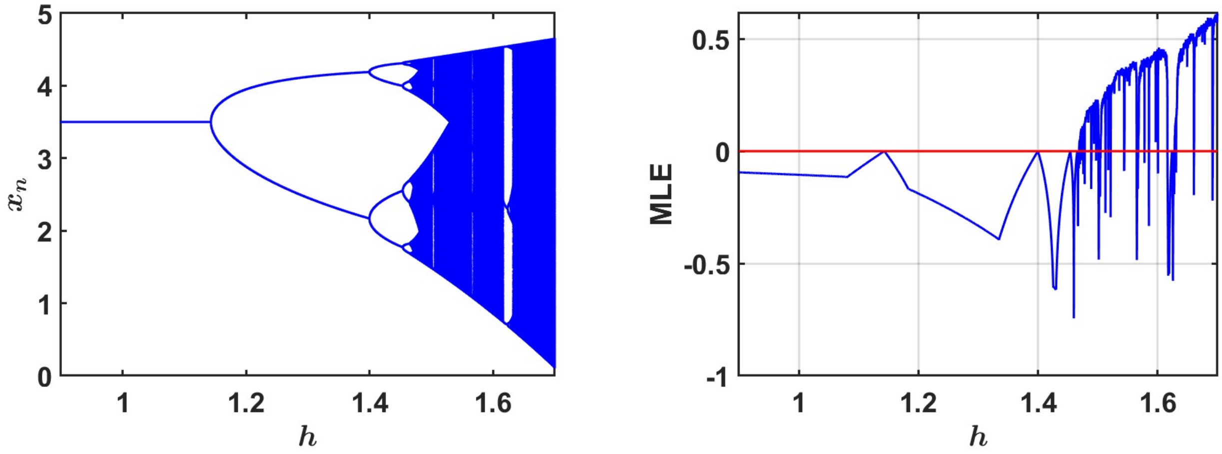

(a) Bifurcation diagram for x_n

(b) Bifurcation diagram for y_n

Figure 3. Bifurcation diagram and MLE plot of (1.2) showing PD bifurcation at E_1 varying $h \in [0.9, 1.7]$. Fixed parameter values are $\alpha = 0.85, \beta = 0.65, \gamma = 1.15, \eta = 0.35, \epsilon = 0.5, r = 2.25$, and $k = 4.5$, and initial values are $x_0 = 3.45, y_0 = 0.01$.

4.3. Bifurcation analysis at E^* varying k

We fix the parameter values $\alpha = 7.4, \beta = 7.2, \gamma = 1.7, \eta = 4.5, \epsilon = 6.5, h = 1.3$, and $r = 8.4$ in order to investigate the effect of the carrying capacity k on the system dynamics. The parameter k has an important ecological significance since it denotes the limitation of the environment in the prey's development. Differences in the values of k can be due to variation in the availability of resources, habitats, and environmental support. In the case of those parameters' values, the critical point of the NS bifurcation will be $k_2 = 4.04318$. The coexistence equilibrium in this scenario will be denoted by $E^* = (0.62963, 0.079987)$. It follows from evaluating the Jacobian matrix at E^* that there exist eigenvalues $\xi_{1,2} = 0.149735 \pm 0.988726i$, which have the modulus of one. Moreover, some careful calculations give

$$\tau_{20} = -1.22528 + 3.95136i,\ \tau_{11} = 4.08977 + 12.65850i,$$
$$\tau_{02} = 5.31505 + 8.70714i,\ \tau_{21} = 0.$$

Thus, it is obtained that $L = -280.79 < 0$, which verifies Theorem 3.5. Thus, NS bifurcation is supercritical, and a closed invariant attracting curve will emerge from E^*.

The bifurcation diagrams in Figures 4(a) and 4(b) depict the dynamical behavior of the prey and predator populations as the parameter k changes. On the other hand, the MLE as illustrated in Figure 4(c) gives a quantitative analysis of the system's stability. In case the value of the MLE is negative, it implies that the dynamics of the system is either stable or quasi-periodic, whereas a positive MLE implies chaos.

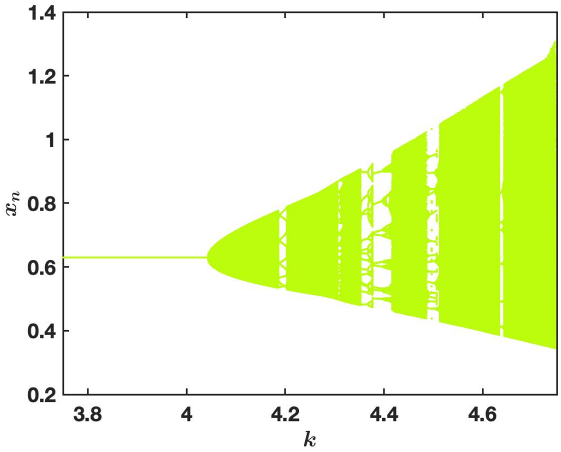

(a) Bifurcation diagram for x_n

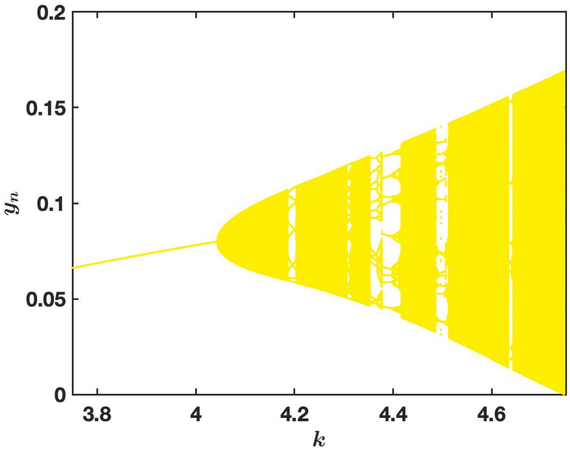

(b) Bifurcation diagram for y_n

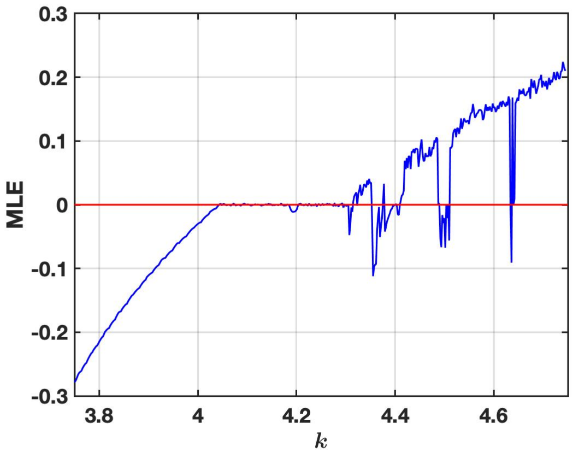

(c) MLE plot

Figure 4. Bifurcation diagrams and MLE plot of (1.2) with respect to k. Parameters are $\alpha = 7.4, \beta = 7.2, \gamma = 1.7, \eta = 4.5, \epsilon = 6.5, h = 1.3$, and $r = 8.4$, with initial values $x_0 = 0.63, y_0 = 0.08$.

The phase portraits for the system (1.2) have been shown in Figures 5(a)–5(i) for various values of k. It is seen that if $k < 4.04318$, then the coexistence equilibrium point E^* is locally asymptotically stable as can be observed from Figure 5(a). For the critical value $k = 4.04318$, an NS bifurcation occurs, and the stability of E^* becomes unstable while an invariant closed curve arises as depicted in Figure 5(b) at $k = 4.1 > k_2$. Further increase in k results in the increase in size of the invariant curve, suggesting oscillation in the populations. This implies that due to an increase in environmental capacity, there will be more fluctuations in prey and predator populations. Next, it is observed that the invariant curve breaks and gives rise to higher periodic orbits like period-9 and period-14 cycles (Figures 5(c) and 5(f)). Eventually, the phase portraits are irregular and aperiodic as shown in Figures 5(e), 5(h), and 5(i).

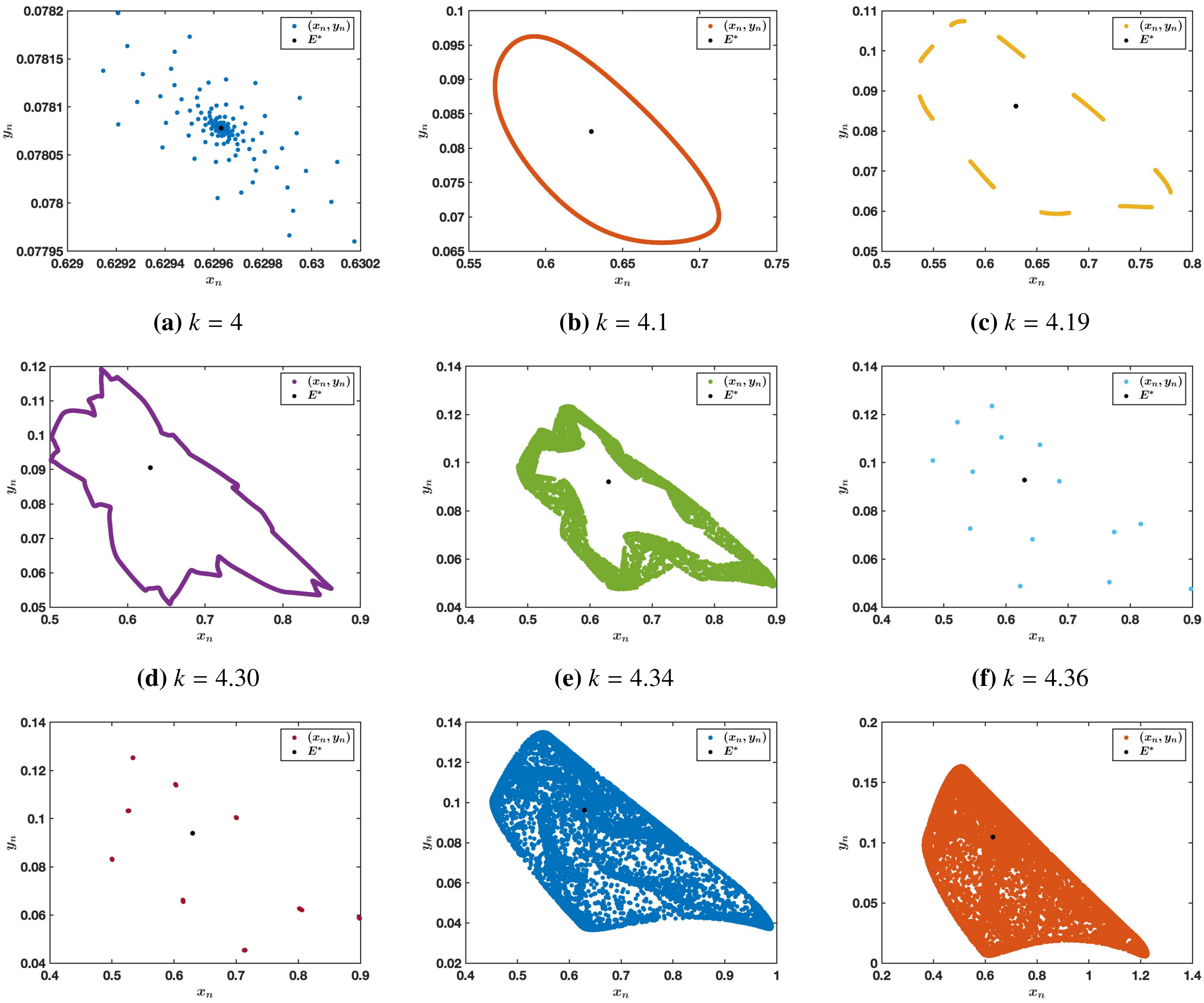

(a) $k = 4$ **(b)** $k = 4.1$ **(c)** $k = 4.19$

(d) $k = 4.30$ **(e)** $k = 4.34$ **(f)** $k = 4.36$

(g) $k = 4.39$ **(h)** $k = 4.45$ **(i)** $k = 4.70$

Figure 5. Phase diagrams of (1.2) for some values of k, with $\alpha = 7.4, \beta = 7.2, \gamma = 1.7, \eta = 4.5, \epsilon = 6.5, h = 1.3$, and $r = 8.4$ and initial values $x_0 = 0.63, y_0 = 0.08$.

Ecologically speaking, these outcomes signify that an increase in the capacity of the environment would not guarantee stability within the system. On the contrary, increasing the value of k could result in large population fluctuations and chaotic dynamics that would render the ecosystem unstable and susceptible to its eventual collapse. This is further complicated by the factors of prey harvesting and anti-predatory behavior.

Parameter values are fixed as $\alpha = 2.3, \beta = 0.8, \gamma = 0.2, \eta = 0.5, \epsilon = 0.6, h = 2.5$, and $r = 2.8$ to study the existence of PD bifurcations varying k. At these parameter values, the threshold for PD bifurcation occurs at $k_1 = 1.728395$. The corresponding positive equilibrium is $E^* = (0.666667, 0.486957)$. Eigenvalues of $J(E^*)$ are $\xi_1 = -1$ and $\xi_2 = 0.3$. Moreover, some careful calculations give $l_1 = 6.00824 \neq 0$ and $l_2 = 163.496 \neq 0$, which verifies Theorem 3.4. Since $l_2 > 0$, a stable orbit of period-2 emanates from E^*. Figures 6(a) and 6(b) illustrate the bifurcation diagram for prey and predator populations, respectively, when k varies between 1.655 and 1.755. It can be seen from the figures that when k crosses k_1, the dynamical behavior changes from a stable fixed point to a stable periodic cycle of order two, which is known as a PD bifurcation. Further change in the parameter value results in a series of doublings. The MLE graph associated with these bifurcation diagrams is given in Figure 6(c).

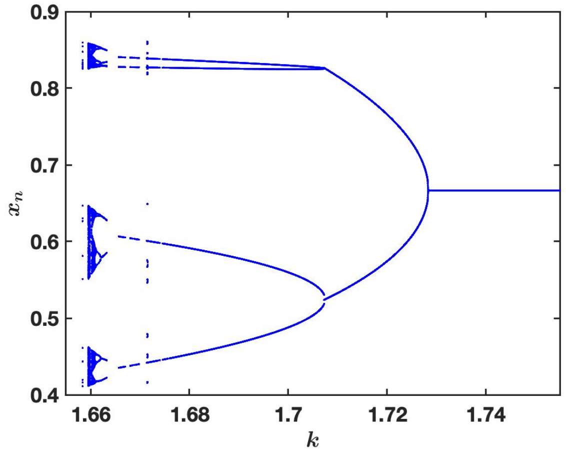

(a) Bifurcation diagram for x_n

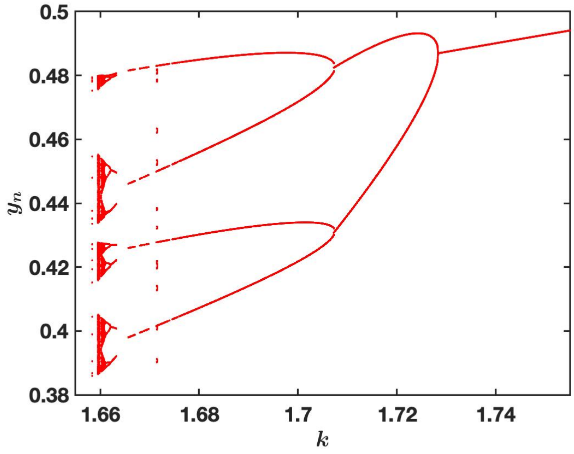

(b) Bifurcation diagram for y_n

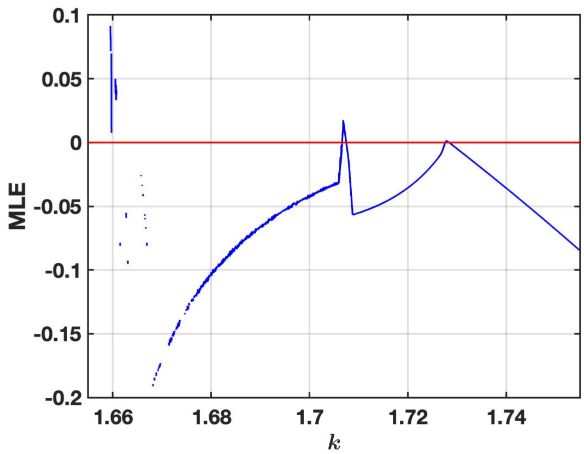

(c) MLE plot

Figure 6. Bifurcation diagrams and MLE plot of (1.2) varying k. Fixed parameter values are $\alpha = 2.3, \beta = 0.8, \gamma = 0.2, \eta = 0.5, \epsilon = 0.6, h = 2.5$, and $r = 2.8$, and initial conditions are $x_0 = 0.6667, y_0 = 0.4870$.

4.4. *Two-parameter analysis*

For further exploration into the global dynamics of this system, a two-parameter bifurcation analysis is carried out. In this technique, one can analyze the effect of interaction between important parameters on qualitative dynamics of the system. Initially, we assume $\alpha = 7.4, \beta = 7.2, \gamma = 1.7, \eta = 4.5, \epsilon = 6.5$, and $h = 1.3$ and vary the values of $k \in [3.75, 4.75]$ and $r \in [8.1, 8.7]$. The above parameters have biological significance, as the value of k determines the ability of the environment to support the prey population, while r determines the growth rate of the prey population.

The two-dimensional bifurcation diagram in terms of (k, r) is shown in Figure 7(a). Colors depict the periodic solutions for various orders of periodicity, while the black areas depict chaos. It is clear from the diagram that for relatively lower values of k and r, the dynamical system lies in a state of stability. This state may be a low-period state or even an equilibrium state. With increasing values of k and r, the system becomes unstable and experiences bifurcations leading to periodic and chaotic states.

The two-dimensional plot for the MLE is illustrated in Figure 7(b). The blue areas represent negative MLE and thus show stable equilibria or periodic orbits. Red areas signify positive MLE and denote chaos. The movement between the light-colored areas is termed quasi-periodicity.

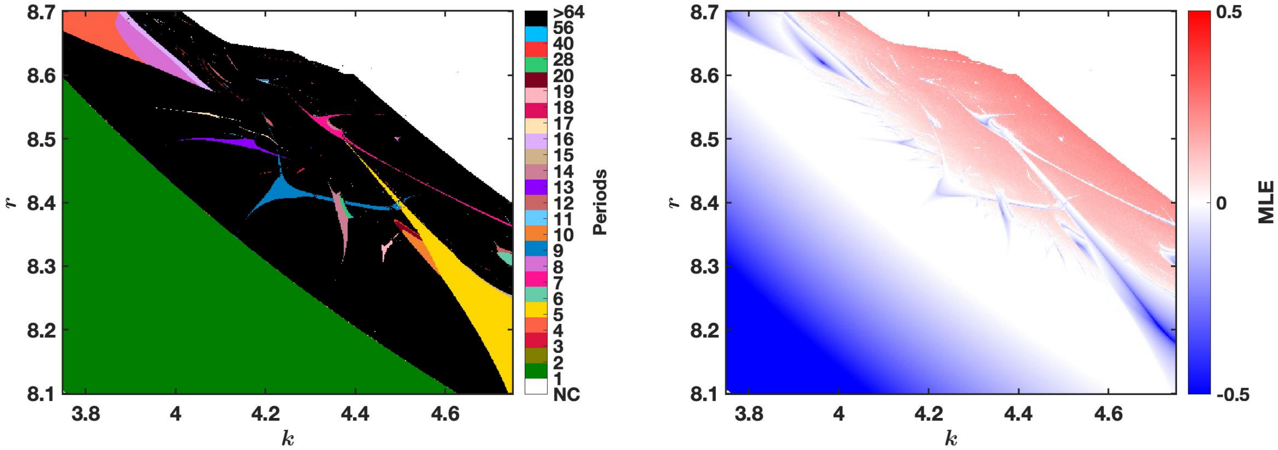

(a) Bifurcation diagram in the (k, r)-plane

(b) MLE plot in the (k, r)-plane

Figure 7. Two-dimensional bifurcation diagram and MLE plot of (1.2) in the (k, r)-plane for $k \in [3.75, 4.75]$ and $r \in [8.1, 8.7]$. Parameters are $\alpha = 7.4, \beta = 7.2, \gamma = 1.7, \eta = 4.5, \epsilon = 6.5$, and $h = 1.3$, with initial values $x_0 = 0.63, y_0 = 0.08$.

Ecologically speaking, the findings suggest that the joint influence of environmental carrying capacity and intrinsic growth rate is important for achieving stability. Stable existence of the species is possible only when these parameters are moderate. Otherwise, large values could lead to oscillations or even chaos, causing instability in the ecology.

Next, we study the effects of the combination of the prey harvesting coefficient ϵ and the anti-predation factor η. In this case, we use the same values of $\alpha = 7.4, \beta = 7.2, \gamma = 1.7, r = 8.8, k = 4.8$, and $h = 1.3$ but change the parameters $\epsilon \in [6.2, 7.4]$ and $\eta \in [3.7, 5.7]$. Figure 8(a) shows the two-dimensional bifurcation plot in the (ϵ, η)-space. From this figure one can see that the dynamics of the system critically depend on the mutual influence of these factors. There exists a rather extensive area, which corresponds to the low-period regular behavior and mostly covers the upper right part of the space where the coefficients ϵ and η take larger values. Thus, one can conclude that for such combinations of parameters, higher values of both prey harvesting and anti-predation coefficients can lead to more regular regimes. For smaller and intermediate values of η, the system is chaotic.

The two-dimensional MLE plot for this figure is illustrated in Figure 8(b), and this plot supports the existence of the bifurcation diagram. The blue shaded areas represent negative MLE values and thus stability, whereas the red shaded areas represent positive MLE values and thus chaos. The transition through different shades of colors represents quasi-periodicity.

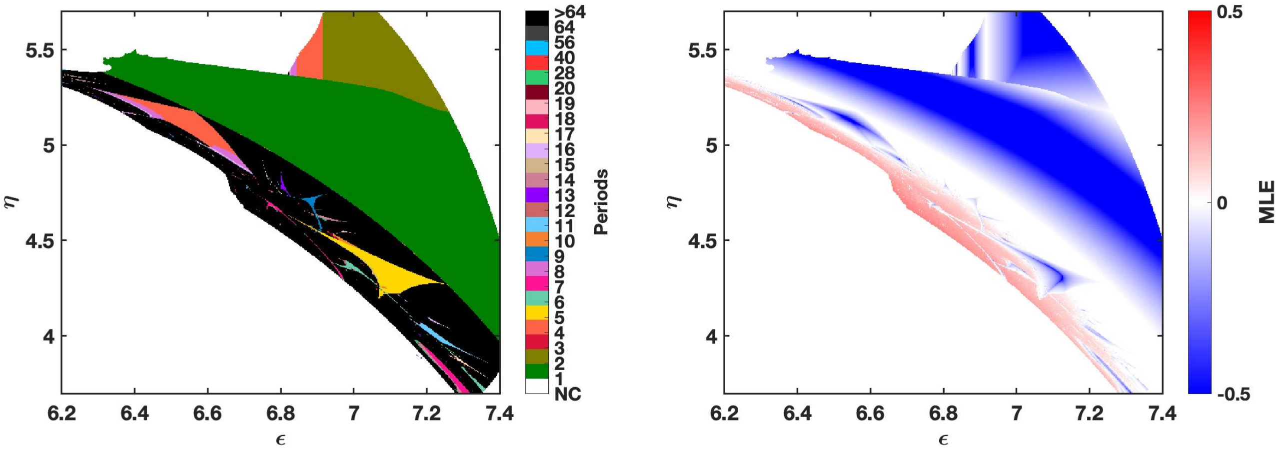

(a) Bifurcation diagram in the (ϵ, η)-plane **(b)** MLE plot in the (ϵ, η)-plane

Figure 8. Two-dimensional bifurcation diagram and MLE plot of (1.2) varying $\epsilon \in [6.2, 7.4]$ and $\eta \in [3.7, 5.7]$. Fixed parameter values are $\alpha = 7.4, \beta = 7.2, \gamma = 1.7, r = 8.8, k = 4.8$, and $h = 1.3$, and initial values are $x_0 = 0.63, y_0 = 0.08$.

Ecologically, the findings reveal that the interplay between prey harvesting and anti-predation significantly affects the stability of the ecosystem. Large values of ϵ and η ensure system stability, resulting in consistent fluctuations of the populations. However, small and medium values of η render the system chaotic, implying that its population undergoes erratic and unpredictable changes. Therefore, achieving an optimal level of prey harvesting and anti-predation is crucial for maintaining ecological stability.

5. Conclusions

This study analyzed a discrete-time predator-prey model incorporating prey harvesting and anti-predator behavior. The discrete model was formulated by applying the forward Euler discretization to a continuous model. This enabled us to study the occurrence of intricate dynamics that cannot be seen in continuous models. The existence and local stability conditions of the equilibrium points, including the biologically feasible coexistence equilibrium, were established through Jacobian and eigenvalue analysis.

A key contribution of this study is the detailed bifurcation analysis of the positive equilibrium. Analytical conditions under which the onset of transcritical, PD, and NS bifurcations may take place were derived, indicating that even slight changes of parameters may lead to qualitative shifts in dynamics of the system. These theoretical findings were also confirmed through numerical simulation. For instance, bifurcation diagrams, phase portraits, and graphs of the MLE illustrated the change in dynamics from stable equilibrium through periodic oscillations, quasi-periodicity, and up to chaos. The findings have shown that an increase in carrying capacity as well as an improper combination of parameters may lead to the destruction of stability.

In contrast to previous studies that mainly examine prey harvesting and anti-predator effects separately or within continuous-time frameworks, this study considers their combined influence in a discrete predator-prey model. The results clarify how the interaction between these two ecological factors affects population stability and the emergence of complex dynamics.

From an ecological perspective, the results emphasize the importance of balancing prey harvesting and anti-predator effects. Excessive harvesting or unfavorable parameter combinations may destabilize population dynamics, whereas appropriate conditions can support stable coexistence.

Author contributions

Asifa Tassaddiq: Conceptualization, Investigation, Methodology, Software, Writing–original draft; Youngsoo Seol: Investigation, Methodology, Supervision, Validation, Writing–review and editing; Rabab Alharbi: Formal analysis, Software, Validation, Writing–review and editing; Ruhaila Md Kasmani: Formal analysis, Software, Validation, Writing–review and editing; Rizwan Ahmed: Conceptualization, Methodology, Supervision, Writing–original draft. All authors have read and approved the final version of the manuscript for publication.

Use of Generative-AI tools declaration

The authors declare they have not used Artificial Intelligence (AI) tools in the creation of this article.

Acknowledgments

The authors extend their appreciation to the Deanship of Postgraduate Studies and Scientific Research at Majmaah University for funding this research work through the project number (ICR-2026-400). This work was supported by the Dong-A University research fund. This research was supported by Global - Learning Academic research institution for Master's-PhD students, and Postdocs (LAMP) Program of the National Research Foundation of Korea (NRF) grant funded by the Ministry of Education (RS-2025-25440216), and by the National Research Foundation of Korea (NRF) grant funded by the Korea government (MSIT) (RS-2026-25480313).

Conflict of interest

The authors declare that there are no conflicts of interest.

References

1. A. J. Lotka, Elements of physical biology, *Nature*, **116** (1925), 461. https://doi.org/10.1038/116461b0

2. V. Volterra, Fluctuations in the abundance of a species considered mathematically, *Nature*, **118** (1926), 558–560. https://doi.org/10.1038/118558a0

3. W. J. Li, L. T. Zhang, J. D. Cao, A note on Turing-Hopf bifurcation in a diffusive Leslie-Gower model with weak Allee effect on prey and fear effect on predator, *Appl. Math. Lett.*, **172** (2025), 109741. https://doi.org/10.1016/j.aml.2025.109741

4. W. J. Li, W. H. Bai, J. D. Cao, Turing instability and pattern formation in a diffusive predator-prey system with opportunistic predators and weak Allee effect, *Phys. Rev. E* , **113** (2026), 044219. https://doi.org/10.1103/5fx7-q41y

5. K. Kayal, S. Samanta, S. Rana, S. Karmakar, J. Chattopadhyay, Impact of predator-driven Allee and spatiotemporal effect on a simple predator-prey model, *Int. J. Bifurcat. Chaos*, **34** (2024), 2450046. https://doi.org/10.1142/S0218127424500469

6. S. Kumar, H. Kharbanda, Chaotic behavior of predator-prey model with group defense and non-linear harvesting in prey, *Chaos Soliton. Fract.*, **119** (2019), 19–28. https://doi.org/10.1016/j.chaos.2018.12.011

7. A. Suryanto, I. Darti, H. S. Panigoro, A. Kilicman, A fractional-order predator-prey model with ratio-dependent functional response and linear harvesting, *Mathematics*, **7** (2019), 1100. https://doi.org/10.3390/math7111100

8. M. G. Mortuja, M. K. Chaube, S. Kumar, Dynamic analysis of a predator-prey system with nonlinear prey harvesting and square root functional response, *Chaos Soliton. Fract.*, **148** (2021), 111071. https://doi.org/10.1016/j.chaos.2021.111071

9. H. S. Panigoro, M. Rayungsari, A. Suryanto, Bifurcation and chaos in a discrete-time fractional-order logistic model with Allee effect and proportional harvesting, *Int. J. Dynam. Control* , **11** (2023), 1544–1558. https://doi.org/10.1007/s40435-022-01101-5

10. M. Imran, M. B. Almatrafi, R. Ahmed, Stability and bifurcation analysis of a discrete predator-prey system of Ricker type with harvesting effect, *Commun. Math. Biol. Neurosci.*, **2024** (2024), 11. https://doi.org/10.28919/cmbn/8313

11. Z. Eskandari, P. A. Naik, M. Yavuz, Dynamical behaviors of a discrete-time prey-predator model with harvesting effect on the predator, *J. Appl. Anal. Comput.*, **14** (2024), 283–297. https://doi.org/10.11948/20230212

12. S. Singh, P. Gupta, A. Priyadarshi, Unveiling multistability and chaos in a discretized predator-prey model incorporating harvesting and refuge: A study of Arnold tongues and shrimp-shaped periodic structures, *Chaos Soliton. Fract.*, **203** (2026), 117639. https://doi.org/10.1016/j.chaos.2025.117639

13. B. Tang, Y. N. Xiao, Bifurcation analysis of a predator-prey model with anti-predator behaviour, *Chaos Soliton. Fract.*, **70** (2015), 58–68. https://doi.org/10.1016/j.chaos.2014.11.008

14. K. D. Prasad, B. S. R. V. Prasad, Qualitative analysis of additional food provided predator-prey system with anti-predator behaviour in prey, *Nonlinear Dyn.*, **96** (2019), 1765–1793. https://doi.org/10.1007/s11071-019-04883-0

15. S. Saha, G. P. Samanta, Effect of anti-predator behaviour in a prey-predator system with strong Allee effect in prey population, *Filomat*, **35** (2021), 4837–4870. https://doi.org/10.2298/fil2114837s

16. B. M. Wang, X. N. Li, Modeling and dynamical analysis of a fractional-order predator-prey system with anti-predator behavior and a Holling type IV functional response, *Fractal Fract.*, **7** (2023), 722. https://doi.org/10.3390/fractalfract7100722

17. T. Wen, Y. C. Xu, M. He, L. B. Rong, Modelling the dynamics in a predator-prey system with Allee effects and anti-predator behavior, *Qual. Theory Dyn. Syst.*, **22** (2023), 116. https://doi.org/10.1007/s12346-023-00821-z

18. R. M. May, Simple mathematical models with very complicated dynamics, *Nature*, **261** (1976), 459–467. https://doi.org/10.1038/261459a0

19. Y. B. Chong, A. J. Kashyap, S. M. Chen, F. D. Chen, Dynamics analysis of a discrete-time commensalism model with additive Allee for the host species, *Axioms*, **12** (2023), 1031. https://doi.org/10.3390/axioms12111031

20. Y. Liu, L. F. Guo, X. J. Liu, Multiple bifurcation analysis in a discrete-time predator-prey model with Holling IV response function, *Symmetry*, **17** (2025), 1459. https://doi.org/10.3390/sym17091459

21. M. B. Almatrafi, M. Berkal, R. Ahmed, Dynamical transitions and chaos control in a discrete predator-prey model with Gompertz growth and Holling type III response, *Chaos Soliton Fract* , **200** (2025), 117071. https://doi.org/10.1016/j.chaos.2025.117071

22. F. Gumusboga, F. Kangalgil, Dynamics of a discrete predator-prey model with an Allee effect in prey: Stability, bifurcation analysis and chaos control, *Int. J. Bifurcat. Chaos*, **35** (2025), 2550097. https://doi.org/10.1142/s021812742550097x

23. R. K. Naji, Contribution of hunting cooperation and antipredator behavior to the dynamics of the harvested prey-predator system, *Commun. Math. Biol. Neurosci.*, **2023** (2023), 99. https://doi.org/10.28919/cmbn/8164

24. R. Kaushik, S. Banerjee, Predator-prey ecological system with group defense and anti-predator traits of the preys: Synergies between two important ecological actions, *Mathematics Open*, **02** (2023), 2350008. https://doi.org/10.1142/s2811007223500086

25. M. X. He, Z. Li, Dynamics of a Holling-Tanner predator-prey model with harvesting and anti-predator behavior, *Appl. Math. Lett.*, **172** (2026), 109732. https://doi.org/10.1016/j.aml.2025.109732

26. S. M. Salman, A. M. Yousef, A. A. Elsadany, Stability, bifurcation analysis and chaos control of a discrete predator-prey system with square root functional response, *Chaos Soliton. Fract.*, **93** (2016), 20–31. https://doi.org/10.1016/j.chaos.2016.09.020

27. A. A. Elsadany, A. M. Yousef, S. A. Ghazwani, A. S. Zaki, Bifurcation analysis of a discrete Basener-Ross population model: Exploring multiple scenarios, *Computation*, **13** (2025), 11. https://doi.org/10.3390/computation13010011

28. M. Rafaqat, A. A. Zubaidi, F. Z. Duraihem, J. Younis, S. T. Saeed, Stability analysis of a discrete-time predator-prey model using piecewise constant argument, *Discrete Dyn. Nat. Soc.*, **2025** (2025), 1566022. https://doi.org/10.1155/ddns/1566022

29. J. Guckenheimer, P. Holmes, *Nonlinear oscillations, dynamical systems, and bifurcations of vector fields*, New York: Springer, 1983. https://doi.org/10.1007/978-1-4612-1140-2

30. S. Wiggins, *Introduction to applied nonlinear dynamical systems and chaos*, 2 Eds., New York: Springer, 2003. https://doi.org/10.1007/b97481

31. Y. A. Kuznetsov, *Elements of applied bifurcation theory*, 3 Eds., New York: Springer, 2004. https://doi.org/10.1007/978-1-4757-3978-7

A. Coefficients corresponding to the nonlinear components of system (3.16)

$$c_1 = -\frac{\alpha(2+h\gamma)(8+4h\gamma-2h^2\gamma^2+h^3\gamma^2(r-\epsilon))}{\gamma(-2+h(r-\epsilon))(-4-4h\gamma+h^2\gamma(r-\epsilon))},\ c_2 = -\frac{h^4\alpha\gamma^2(-2+h(r-\epsilon))(r+\gamma-\epsilon)}{2(2+h\gamma)(-4-4h\gamma+h^2\gamma(r-\epsilon))},$$

$$c_3 = -\frac{h\alpha(2+h\gamma)(4+h^2\gamma(r-\epsilon))}{-8-8h\gamma+2h^2\gamma(r-\epsilon)},\ c_4 = -\frac{(4+h^2\gamma(r-\epsilon))^2(\beta-\eta)}{hr\gamma(-4-4h\gamma+h^2\gamma(r-\epsilon))},$$

$$c_5 = -\frac{(-2+h(r-\epsilon))(4+h^2\gamma(r-\epsilon))^2(\beta-\eta)}{2r(2+h\gamma)(-4-4h\gamma+h^2\gamma(r-\epsilon))},\ c_6 = \frac{2\alpha(4+h^2\gamma(r-\epsilon))^2(\beta-\eta)}{hr\gamma^2(-2+h(r-\epsilon))(-4-4h\gamma+h^2\gamma(r-\epsilon))},$$

$$c_7 = \frac{h\alpha(-2+h(r-\epsilon))(4+h^2\gamma(r-\epsilon))^2(\beta-\eta)}{2r(2+h\gamma)^2(-4-4h\gamma+h^2\gamma(r-\epsilon))},\ c_8 = \frac{(4+h^2\gamma(r-\epsilon))^3(\beta-\eta)^2}{h^2r^2\gamma^2(2+h\gamma)(-4-4h\gamma+h^2\gamma(r-\epsilon))},$$

$$c_9 = \frac{(-2+h(r-\epsilon))(4+h^2\gamma(r-\epsilon))^3(\beta-\eta)^2}{2hr^2\gamma(2+h\gamma)^2(-4-4h\gamma+h^2\gamma(r-\epsilon))},\ c_{10} = \frac{2\alpha(4+h^2\gamma(r-\epsilon))^2(\beta-\eta)}{r\gamma(2+h\gamma)(-4-4h\gamma+h^2\gamma(r-\epsilon))},$$

$$d_1 = \frac{2\alpha(2+h\gamma)^3}{\gamma(-2+h(r-\epsilon))(-4-4h\gamma+h^2\gamma(r-\epsilon))},\ d_2 = \frac{h^2\alpha\gamma(8+12h\gamma+h^3\gamma(r-\epsilon)^2+2h^2\gamma(-2r+\gamma+2\epsilon))}{2(2+h\gamma)(-4-4h\gamma+h^2\gamma(r-\epsilon))},$$

$$d_3 = \frac{h^2\alpha(4+h^2\gamma(r-\epsilon))(r+\gamma-\epsilon)}{(-2+h(r-\epsilon))(-4-4h\gamma+h^2\gamma(r-\epsilon))},\ d_4 = \frac{2(4+h^2\gamma(r-\epsilon))^2(r+\gamma-\epsilon)(\beta-\eta)}{r\gamma(2+h\gamma)(-2+h(r-\epsilon))(-4-4h\gamma+h^2\gamma(r-\epsilon))},$$

$$d_5 = \frac{h(4+h^2\gamma(r-\epsilon))^2(r+\gamma-\epsilon)(\beta-\eta)}{r(2+h\gamma)^2(-4-4h\gamma+h^2\gamma(r-\epsilon))},\ d_6 = -\frac{2\alpha(4+h^2\gamma(r-\epsilon))^2(\beta-\eta)}{hr\gamma^2(-2+h(r-\epsilon))(-4-4h\gamma+h^2\gamma(r-\epsilon))},$$

$$d_7 = -\frac{h\alpha(-2+h(r-\epsilon))(4+h^2\gamma(r-\epsilon))^2(\beta-\eta)}{2r(2+h\gamma)^2(-4-4h\gamma+h^2\gamma(r-\epsilon))},\ d_8 = -\frac{2(4+h^2\gamma(r-\epsilon))^3(r+\gamma-\epsilon)(\beta-\eta)^2}{hr^2\gamma^2(2+h\gamma)^2(-2+h(r-\epsilon))(-4-4h\gamma+h^2\gamma(r-\epsilon))},$$

$$d_9 = -\frac{(4+h^2\gamma(r-\epsilon))^3(r+\gamma-\epsilon)(\beta-\eta)^2}{r^2\gamma(2+h\gamma)^3(-4-4h\gamma+h^2\gamma(r-\epsilon))},\ d_{10} = -\frac{2\alpha(4+h^2\gamma(r-\epsilon))^2(\beta-\eta)}{r\gamma(2+h\gamma)(-4-4h\gamma+h^2\gamma(r-\epsilon))}.$$

AIMS Press